

On the choice of beam polarization in $e^+e^- \rightarrow ZZ/Z\gamma$ and anomalous triple gauge-boson couplings

Rafiqul Rahaman^{a,1}, Ritesh K. Singh^{b,1}

¹Department of Physical Sciences, Indian Institute of Science Education and Research Kolkata, Mohanpur, 741246, India

Abstract The anomalous trilinear gauge couplings of Z and γ are studied in $e^+e^- \rightarrow ZZ/Z\gamma$ with longitudinal beam polarizations using a complete set of polarization asymmetries for the Z boson. We quantify the goodness of the beam polarization in terms of the likelihood and find the best-choice of e^- and e^+ polarizations to be $(+0.16, -0.16)$, $(+0.09, -0.10)$ and $(+0.12, -0.12)$ for $ZZ, Z\gamma$ and combined processes, respectively. Simultaneous limits on anomalous couplings are obtained for these choices of beam polarizations using Markov-Chain-Monte-Carlo (MCMC) for an e^+e^- collider running at $\sqrt{s} = 500$ GeV and $\mathcal{L} = 100 \text{ fb}^{-1}$. We find the simultaneous limits for these beam polarizations to be comparable with each other and also comparable with the unpolarized beam case.

1 Introduction

The gauge boson sector in the Standard Model (SM) remains uncharted even after the discovery of Higgs boson [1] at LHC. Of the gauge-boson self couplings (trilinear and quartic), the gauge boson couplings to Higgs, the Higgs self couplings, which are the key to understand Electro Weak Symmetry Breaking (EWSB), there have no precise measurements and they need serious attention. The future International Linear Collider (ILC) [2–4] will be a precision testing machine [5] which will have the possibility of polarized initial beams. Two types of polarization, namely longitudinal and transverse, for both initial beams (e^- and e^+) will play an important role in precise measurement of various parameters, like the coupling among gauge bosons, Higgs coupling to the top quark, and Higgs coupling to the gauge boson. Beam polarization has the ability to enhance the relevant signal to background ratio along with the sensitivity of observables [5–9]. It can

also be used to separate CP-violating couplings from a CP-conserving one [5, 10–19] if CP-violation is present in Nature. These potentials of the beam polarizations have been explored, for example, to study τ polarization [11], top quark polarization [20] and its anomalous couplings [21], littlest Higgs model [22], WWV couplings [6, 7, 23], Higgs couplings to gauge bosons [24–27].

Here we use beam polarizations (longitudinal only) to study anomalous trilinear gauge-boson self couplings in the neutral sector using the complete set of polarization observables of the Z boson [28–30] in the process $e^+e^- \rightarrow ZZ/Z\gamma$. The anomalous couplings among the neutral gauge boson have been studied earlier with unpolarized beam in [31–39] as well as with polarized beams in [15–17, 19, 40–45]. Some of these studies have used given beam polarizations to enhance the sensitivity of observables, while others have used two different sets of beam polarizations to construct the observables. We follow the former method and quantify the likelihood-based goodness of the choice of beam polarizations.

For the process of interest the anomalous triple gauge-boson couplings is given by the Lagrangian [28, 42]

$$\begin{aligned} \mathcal{L} = \frac{g_e}{M_Z^2} & \left[[f_4^Z(\partial_\mu Z^{\mu\beta}) - f_4^\gamma(\partial_\mu F^{\mu\beta})] Z_\alpha (\partial^\alpha Z_\beta) \right. \\ & + [f_5^\gamma(\partial^\sigma F_{\sigma\mu}) + f_5^Z(\partial^\sigma Z_{\sigma\mu})] \tilde{Z}^{\mu\beta} Z_\beta \\ & - [h_1^\gamma(\partial^\sigma F_{\sigma\mu}) + h_1^Z(\partial^\sigma Z_{\sigma\mu})] Z_\beta F^{\mu\beta} \\ & \left. - [h_3^\gamma(\partial_\sigma F^{\sigma\rho}) + h_3^Z(\partial_\sigma Z^{\sigma\rho})] Z^\alpha \tilde{F}_{\rho\alpha} \right]. \end{aligned} \quad (1)$$

The coupling f_i^V 's appear in the ZZ process while h_i^V 's appear in $Z\gamma$ process. Among these couplings f_4^V and h_1^V are CP -odd while others are CP -even. The best limits on these anomalous couplings coming from LHC are $|f_i^V| \sim 3 \times 10^{-3}$ [46] and $|h_i^V| \sim 9 \times 10^{-4}$ [47].

^aemail:rr13rs033@iiserkol.ac.in

^bemail:ritesh.singh@iiserkol.ac.in

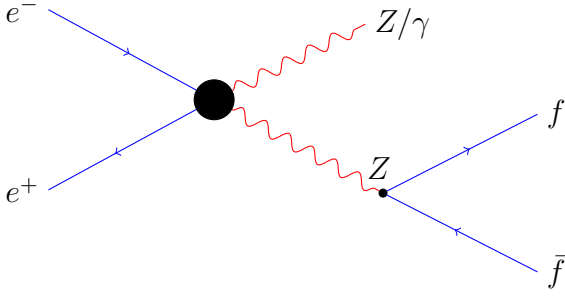


Fig. 1 Feynman diagram for production of Z boson and its decay to a pair of fermions

The rest of the paper is organized as follows. In [section 2](#) we discuss basic formulations and the Z boson polarization observables. In [section 3](#) we study beam polarization dependence of sensitivity and likelihood. We define a *measure of goodness* for the choice of beam polarizations and study ZZ/Z γ processes to obtain the best choices. The simultaneous limits are presented for a set of beam polarizations. We conclude in [section 4](#).

2 Beam polarization and polarization observables

The polarization density matrices for e^- and e^+ beams are given by

$$P_{e^-}(\lambda_{e^-}, \lambda'_{e^-}) = \frac{1}{2} \begin{bmatrix} (1 + \eta_3) & \eta_T \\ \eta_T & (1 - \eta_3) \end{bmatrix} \quad \text{and} \quad (2)$$

$$P_{e^+}(\lambda_{e^+}, \lambda'_{e^+}) = \frac{1}{2} \begin{bmatrix} (1 + \xi_3) & \xi_T e^{-i\delta} \\ \xi_T e^{i\delta} & (1 - \xi_3) \end{bmatrix}, \quad (3)$$

where η_3 and η_T (ξ_3 and ξ_T) are longitudinal and transverse polarization of e^- (e^+) with δ being the azimuthal angle between two transverse polarizations. The positive x -axis is taken along the transverse polarization of e^- and positive z -axis along its momentum.

The density matrix for the production of Z boson in the above process (Fig. 1) would be

$$\rho(\lambda_Z, \lambda'_Z) = \sum_{\lambda_{e^-}, \lambda'_{e^-}, \lambda_{e^+}, \lambda'_{e^+}} \mathcal{M}^\dagger(\lambda'_{e^-}, \lambda'_{e^+}, \lambda'_Z) \times \mathcal{M}(\lambda_{e^-}, \lambda_{e^+}, \lambda_Z) \times P_{e^-}(\lambda_{e^-}, \lambda'_{e^-}) \times P_{e^+}(\lambda_{e^+}, \lambda'_{e^+}). \quad (4)$$

We note that the different helicities can take the following values:

$$\lambda_Z, \lambda'_Z \in \{-1, 0, 1\} \quad \text{and} \quad \lambda_{e^\pm}, \lambda'_{e^\pm} \in \{-1, 1\}. \quad (5)$$

For the present work we restrict ourselves only to the longitudinal beam polarizations, i.e. $\eta_T = 0 = \xi_T$. With the chosen beam polarizations we construct the complete set of eight polarization observables for the Z boson along with total cross section in the processes $e^+e^- \rightarrow ZZ/Z\gamma$. These polarization observables can be obtained

analytically from the production process as well as from asymmetries constructed from decay distribution of the particle. The polarization observables consist of a 3 component vector polarization $\mathbf{P} \equiv (P_x, P_y, P_z)$ and a traceless symmetric rank-2 tensor $T_{ij}(i, j = x, y, z)$ with 5 independent component $T_{xy}, T_{xz}, T_{yz}, T_{xx} - T_{yy}$ and T_{zz} . The asymmetries in the collider or in a Monte Carlo event generator corresponding to P_i 's and T_{ij} 's are $\{A_x, A_y, A_z\}$ and $\{A_{xy}, A_{xz}, A_{yz}, A_{x^2-y^2}, A_{zz}\}$, respectively. The asymmetries A_z, A_{xz}, A_{yz} are zero in SM and even with polarized beam in both processes owing to the forward-backward symmetry of produced Z in these processes. To make these asymmetries non-zero we redefine the polarization observables $\mathcal{O} \in \{P_z, T_{xz}, T_{yz}\}$ as

$$\mathcal{O} \rightarrow \tilde{\mathcal{O}} = \frac{1}{\sigma_Z} \left[\int_0^{c_{\theta_0}} \text{Comb}(\mathcal{O}, \rho(\lambda, \lambda')) dc_{\theta_Z} - \int_{-c_{\theta_0}}^0 \text{Comb}(\mathcal{O}, \rho(\lambda, \lambda')) dc_{\theta_Z} \right], \quad (6)$$

where c_{θ_0} is the beam pipe cut and $\text{Comb}(\mathcal{O}, \rho(\lambda, \lambda'))$ is the combination of production density matrix corresponding the polarization observable \mathcal{O} (see Ref. [28]). For example, with $\mathcal{O} = P_z$ one has

$$\text{Comb}(P_z, \rho(\lambda, \lambda')) = \rho(+1, +1) - \rho(-1, -1)$$

and the corresponding modified polarization is given by

$$\tilde{P}_z = \frac{1}{\sigma_Z} \left[\int_0^{c_{\theta_0}} \left[\rho(+1, +1) - \rho(-1, -1) \right] dc_{\theta_Z} - \int_{-c_{\theta_0}}^0 \left[\rho(+1, +1) - \rho(-1, -1) \right] dc_{\theta_Z} \right]. \quad (7)$$

The asymmetries \tilde{A}_z corresponding to the modified polarization \tilde{P}_z is given by:

$$\tilde{A}_z \equiv \frac{1}{\sigma} \left(\sigma(c_{\theta_Z} \times c_{\theta_f} > 0) - \sigma(c_{\theta_Z} \times c_{\theta_f} < 0) \right). \quad (8)$$

Similarly A_{xz} and A_{yz} related to T_{xz} and T_{yz} are modified as

$$\tilde{A}_{xz} \equiv \frac{1}{\sigma} \left(\sigma(c_{\theta_Z} \times c_{\theta_f} c_{\phi_f} > 0) - \sigma(c_{\theta_Z} \times c_{\theta_f} c_{\phi_f} < 0) \right),$$

$$\tilde{A}_{yz} \equiv \frac{1}{\sigma} \left(\sigma(c_{\theta_Z} \times c_{\theta_f} s_{\phi_f} > 0) - \sigma(c_{\theta_Z} \times c_{\theta_f} s_{\phi_f} < 0) \right). \quad (9)$$

Redefining these asymmetries increases the total number of the non-vanishing observables to put simultaneous limit on the anomalous coupling and we expect limits tighter than reported earlier in Ref. [28].

The total cross section (or total number of events) of a process plays an important role determining the sensitivity and the limits on the anomalous couplings. A tighter limit on the anomalous couplings can be obtained if the cross section can be enhanced. Beam polarization can enhance the cross

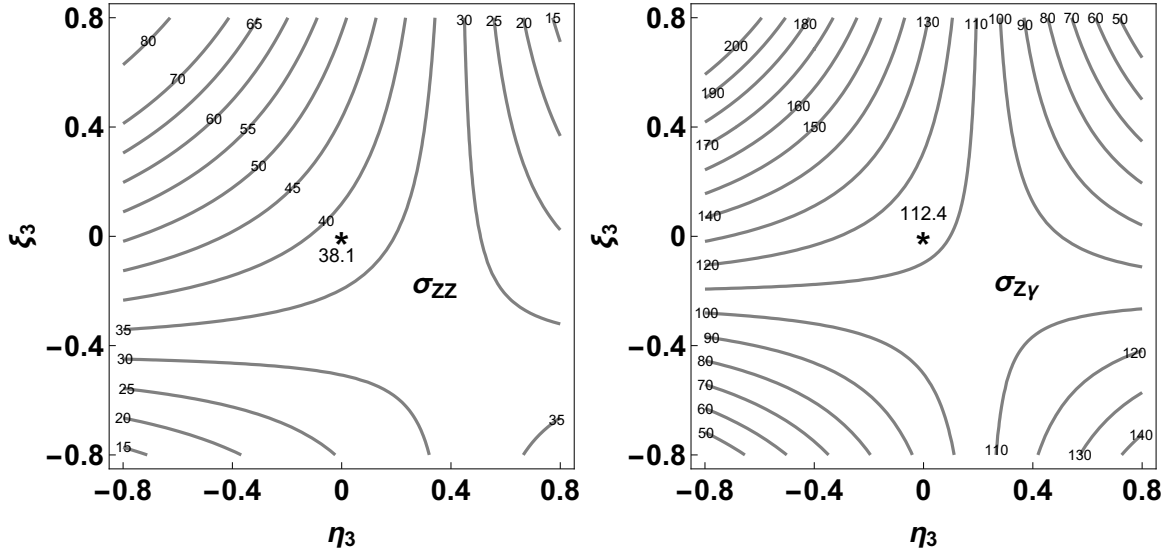


Fig. 2 The SM cross section (in fb) for the process $e^+e^- \rightarrow ZZ/Z\gamma$ as a function of longitudinal beam polarizations η_3 (for e^-) and ξ_3 (for e^+) at $\sqrt{s} = 500$ GeV

section and hence it is important to see how it depends on beam polarization. Fig. 2 shows the dependence of the cross sections σ_{ZZ} and $\sigma_{Z\gamma}$ on the longitudinal beam polarizations η_3 and ξ_3 at $\sqrt{s} = 500$ GeV. The asterisk mark on the middle of the plots represents the unpolarized case. We notice that the cross section in the two processes are larger for negative value of η_3 and positive value of ξ_3 . The sensitivity on the cross section is expected to be high in the left-top corner of the $\eta_3 - \xi_3$ plane. This would convince us to set beam polarizations at the left-top corner for analysis. But the cross section is not the only observable, the asymmetries have different behaviour on beam polarizations. For example, A_x peaks at the right-bottom corner, i.e. we have an opposite behaviour compared to cross section, while A_z has a similar dependence as cross section on the beam polarizations in both the processes. Processes involving W^\pm are also expected to have higher cross section at the left-top corner of $\eta_3 - \xi_3$ plane as W couple to the left chiral electron. Anomalous couplings are expected to change the dependence of all the observables, including the cross section, on the beam polarizations. To explore this we study the effect of beam polarizations on sensitivity of cross section and other observables to anomalous couplings in the next section.

3 Sensitivity, likelihood and the choice of beam polarizations

The sensitivity of an observables \mathcal{O} depending on anomalous couplings \mathbf{f} with a given beam polarizations η_3 and ξ_3 is given by

$$\mathcal{S}(\mathcal{O}(\mathbf{f}, \eta_3, \xi_3)) = \frac{|\mathcal{O}(\mathbf{f}, \eta_3, \xi_3) - \mathcal{O}(\mathbf{0}, \eta_3, \xi_3)|}{|\delta\mathcal{O}(\eta_3, \xi_3)|}, \quad (10)$$

where $\delta\mathcal{O} = \sqrt{(\delta\mathcal{O}_{stat.})^2 + (\delta\mathcal{O}_{sys.})^2}$ is the estimated error in \mathcal{O} . The estimated error to cross section would be

$$\delta\sigma(\eta_3, \xi_3) = \sqrt{\frac{\sigma(\eta_3, \xi_3)}{\mathcal{L}} + \varepsilon_\sigma^2 \sigma(\eta_3, \xi_3)^2}, \quad (11)$$

whereas the estimated error to the asymmetries would be

$$\delta A(\eta_3, \xi_3) = \sqrt{\frac{1 - A(\eta_3, \xi_3)^2}{\mathcal{L} \sigma(\eta_3, \xi_3)} + \varepsilon_A^2}. \quad (12)$$

Here \mathcal{L} is the integrated luminosity, ε_σ and ε_A are the systematic fractional error in cross section and asymmetries, respectively. In these analyses we take $\mathcal{L} = 100 \text{ fb}^{-1}$, $\varepsilon_\sigma = 0.02$ and $\varepsilon_A = 0.01$ as a benchmark.

We study the sensitivity of all the observables and their dependence on the beam polarizations at $\sqrt{s} = 500$ GeV. Choosing a benchmark value for the anomalous couplings to be

$$\mathbf{f} = \{f_4^Y, f_4^Z, f_5^Y, f_5^Z\} = \{+3, +3, +3, +3\} \times 10^{-3},$$

we show the sensitivities for σ , A_{xy} and \tilde{A}_{yz} in Fig. 3 as a function of beam polarizations. The sensitivities for cross section and \tilde{A}_{yz} peak at the left-top corner of the plots. For A_{xy} sensitivity peak at the right-bottom corner, it is not much smaller in the left-top corner either. The sensitivities of all other asymmetries (not shown here) except \tilde{A}_z peaks at the left-top corner although the exact dependence on the beam polarization may differ. Thus, the combined sensitivity of all the observables is high on the left-top corner of the polarization plane making $(\eta_3, \xi_3) = (-0.8, +0.8)$ the best-choice for the chosen benchmark coupling. This best-choice, however, strongly depends upon the values of the anomalous couplings. We note that the best-choice of the beam polarization is mainly decided by

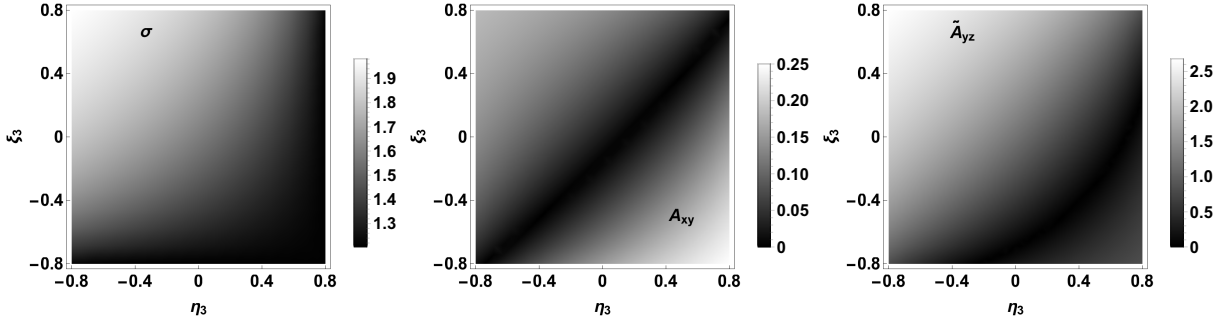


Fig. 3 Effect of beam polarizations on sensitivity of cross section σ , A_{xy} and \tilde{A}_{yz} in the process $e^+e^- \rightarrow ZZ$ for anomalous couplings $\mathbf{f} = \{+3, +3, +3, +3\} \times 10^{-3}$ at $\sqrt{s} = 500$ GeV and $\mathcal{L} = 100 \text{ fb}^{-1}$

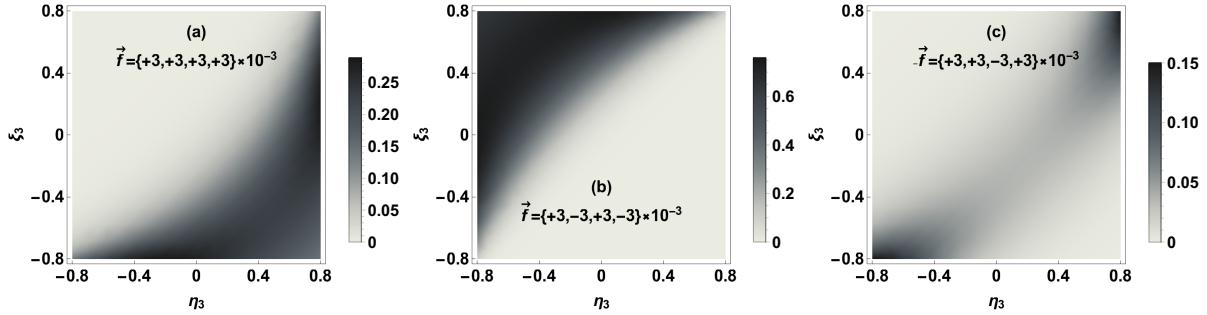


Fig. 4 Likelihood $L(\{\mathcal{O}\}, \mathbf{f}; \eta_3, \xi_3)$ for three different benchmark anomalous couplings at $\sqrt{s} = 500$ GeV and $\mathcal{L} = 100 \text{ fb}^{-1}$ in ZZ process

the behaviour of the cross section because most of the asymmetries also have similar dependences on the beam polarizations. This, however, does not mean that the cross section provides a best sensitivity or the limits. For example, in Fig. 3 we can see that \tilde{A}_{yz} has a better sensitivity than the cross section. For the $Z\gamma$ process with the benchmark point

$$\mathbf{h} = \{h_1^\gamma, h_1^Z, h_3^\gamma, h_3^Z\} = \{+3, +3, +3, +3\} \times 10^{-3}$$

one obtains similar conclusions: the sensitivities of all observables peak at left-top corner of $\eta_3 - \xi_3$ plane (not shown) except for \tilde{A}_z .

For a complete analysis we need to use all the observables simultaneously. To this end we define a likelihood function considering the set of all the observables depending on the anomalous coupling \mathbf{f} as

$$L(\{\mathcal{O}\}, \mathbf{f}; \eta_3, \xi_3) = \exp \left[-\frac{1}{2} \sum_i \mathcal{S}(\mathcal{O}_i(\mathbf{f}, \eta_3, \xi_3))^2 \right], \quad (13)$$

i runs over the set of observables in a process. Maximum sensitivity of observables requires the likelihood to be minimum. The likelihood defined here is proportional to the p -value and hence the best-choice of beam polarizations comes from the *minimum* likelihood or maximum distinguishability.

The beam polarization dependence of the likelihood for the ZZ process at the above chosen anomalous couplings is given in Fig. 4(a). The minimum of the likelihood falls in the left-top corner of the $\eta_3 - \xi_3$ plane as expected as

most of the observables has higher sensitivity at this corner. For different anomalous couplings the minimum likelihood changes its position in the $\eta_3 - \xi_3$ plane. We have checked the likelihood for 16 different corners of

$$\mathbf{f}_{\pm\pm\pm\pm} = \{\pm 3, \pm 3, \pm 3, \pm 3\} \times 10^{-3}$$

and they have different dependences on η_3, ξ_3 . Here we present the likelihood for three different choices of the anomalous couplings in Fig. 4. In Fig. 4(b), the minimum of the likelihood falls in the right-bottom corner where most of the observables have higher sensitivity. In Fig. 4(c) low likelihood falls in both diagonal corners in the $\eta_3 - \xi_3$ plane. This is because some of the observables prefer the left-top corner, while others prefer the right-bottom corner of the polarization plane for higher sensitivity. We have a similar behaviour for the likelihood in the $Z\gamma$ process.

As the anomalous couplings change, the minimum likelihood region changes accordingly and hence the best-choice of beam polarizations. So the best-choice for the beam polarizations depends on the new physics in the process. If one knows the new physics one could tune the beam polarizations to have the best sensitivity for the analysis. But in order to have a suitable choice of beam polarizations irrespective of the possible new physics one needs to minimize the likelihood averaged over all the anomalous couplings. The likelihood function averaged over a volume in parameter space V_f would be defined as

$$L(V_f, \{\mathcal{O}\}; \eta_3, \xi_3) = \int_{V_f} L(\{\mathcal{O}\}, \mathbf{f}; \eta_3, \xi_3) d\mathbf{f}. \quad (14)$$

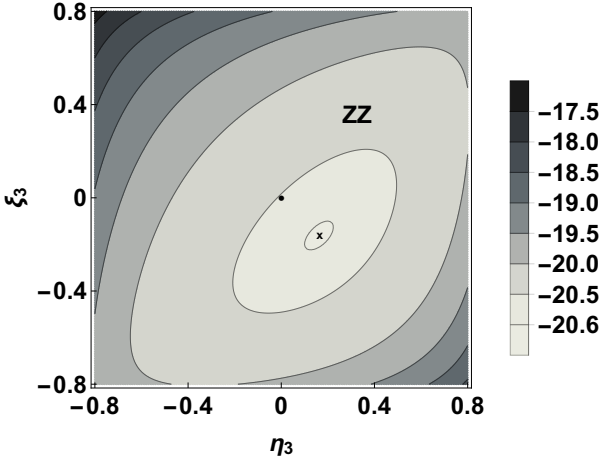


Fig. 5 The log of average likelihood, $\log[L(V_{\mathbf{f}}, \{\mathcal{O}\}; \eta_3, \xi_3)]$ as a function of beam polarization is shown for the ZZ process at $\sqrt{s} = 500$ GeV and $\mathcal{L} = 100 \text{ fb}^{-1}$. The dot at the centre is the $(0,0)$ point, while cross mark at $P_{ZZ} = (+0.16, -0.16)$ is the minimum likelihood point and hence the best-choice of beam polarizations for ZZ process

This quantity is nothing but the *weighted volume* of the parameter space that is statistically consistent with the SM. The size of this weighted volume determines the limits on the parameters. The beam polarizations with the minimum averaged likelihood (or minimum weighted volume) is expected to be the average best choice for any new physics in the process. For numerical analysis we choose the volume to be a hypercube in the 4 dimensional parameter space with sides equal to 2×0.05 (much larger than the available limits on them) in both the processes. The contribution to the average likelihood from the region outside this volume is negligible.

The average likelihood $L(V_{\mathbf{f}}, \{\mathcal{O}\}; \eta_3, \xi_3)$ in the ZZ process as a function of beam polarization is shown in Fig. 5 on log-scale. The dot on the middle of the plot represents the unpolarized case and the cross mark at $P_{ZZ} = (+0.16, -0.16)$ represents the minimum averaged likelihood point i.e., the best-choice of beam polarizations. The unpolarized point, the best point and the points within two central contour in Fig. 5 have the same order of average likelihood and expected to give similar limits on anomalous couplings. The polarization point from darker contours corresponds to larger values of average likelihood and expected to give relatively looser limits on anomalous couplings. To explore this we estimate simultaneous limits using Markov-Chain-Monte-Carlo (MCMC) method at P_{ZZ} , unpolarized beam and few other benchmark choice of beam polarizations. The limits thus obtained on the anomalous couplings for the ZZ process are listed in Table 1. We note that the limits for the best-choice of polarizations (P_{ZZ}) are best but comparable to other nearby benchmark beam polarization including the unpolarized beams. This is due to the fact that the average likelihood is comparable for these

cases. Further, the limits for $(+0.4, -0.4)$ and $(-0.4, +0.4)$ are increasingly bad as these points correspond to the third and fourth contours, i.e., we have increasingly larger average likelihood. The point $(-0.8, +0.8)$ has the largest average likelihood and the corresponding limits are the worst in Table 1. We also note that the limits for the unpolarized case in Table 1 are better than the ones reported in Ref. [28], when adjusted for the systematic errors. This improvement here is due to the inclusion of three new non-vanishing asymmetries \tilde{A}_z , \tilde{A}_{xz} and \tilde{A}_{yz} . Of these, \tilde{A}_{xz} has linear dependence on $f_5^{\gamma,Z}$ with larger sensitivity to f_5^Z leading to about 30 % improvement in the limit. Similarly, the CP-odd asymmetry \tilde{A}_{yz} has a linear dependence on $f_4^{\gamma,Z}$ with larger sensitivity to f_4^Z and this again leads to about 30 % improvement in the corresponding limit. The asymmetry \tilde{A}_z has a quadratic dependence on all four parameters and has too poor sensitivity for all of them to be useful.

We do a similar analysis for the Z γ process. The average likelihood $L(V_{\mathbf{h}}, \{\mathcal{O}\}; \eta_3, \xi_3)$ is shown in Fig. 6 on log-scale. Here also the dot on the middle of the plot is for unpolarized case while the plus mark at $P_{Z\gamma} = (+0.09, -0.10)$ is for the minimum averaged likelihood and hence the best-choice of beam polarizations. The corresponding simultaneous limits on the anomalous couplings h_i are presented in Table 2. Again we notice that the limits obtained for the best-choice of the beam polarizations $P_{Z\gamma}$ are tighter than any other point on the polarization plane, yet comparable to the nearby polarization points within the two central contours in Fig. 6, including the unpolarized point. This again is due to the comparable values of the averaged likelihood of the two central contours containing $P_{Z\gamma}$ and the unpolarized point. The limits at the points $(+0.4, -0.4)$ and $(-0.4, +0.4)$ are worse as they fall in the fourth and fifth contour containing much larger likelihood values. Like the ZZ case the point $(-0.8, +0.8)$ has the largest average likelihood and the corresponding limits are the worst. The simultaneous limits for the unpolarized case (also the $P_{Z\gamma}$) turns out to be much better than the ones reported in Ref. [28] for $h_{1,3}^\gamma$ due to the inclusions of new asymmetries in the present analysis. The CP-odd asymmetry \tilde{A}_{yz} has linear dependence on $h_1^{\gamma,Z}$ with a large sensitivity towards h_1^γ leading to an improvement in the corresponding limit by a factor of two compare to earlier report when adjusted for systematic errors. The limit on h_3^γ improves by a factor of 3 owing to the asymmetry \tilde{A}_{xz} . The limits on $h_{1,3}^Z$ remain comparable.

The combined analysis of the processes ZZ and Z γ is expected to change the best-choice of beam polarizations and limits accordingly. For the average likelihood for these two processes the volume, in which one should average, will change to $V_{\mathbf{f}/\mathbf{h}} \rightarrow V_{\mathbf{F}}$, where $\mathbf{F} = \{\mathbf{f}, \mathbf{h}\}$ and observables from both processes should be added to the likelihood defined

Table 1 List of simultaneous limits on anomalous couplings obtained for $\sqrt{s} = 500$ GeV and $L = 100$ fb $^{-1}$ for different η_3 and ξ_3 from MCMC in ZZ process

Beam polarizations	Limits on couplings (10^{-3})								Comments
	f_4^γ		f_4^Z		f_5^γ		f_5^Z		
(η_3, ξ_3)	68 %	95 %	68 %	95 %	68 %	95 %	68 %	95 %	
-0.80, +0.80	+7.3 -9.3	+13.0 -12.0	+15.0 -14.0	+18.0 -19.0	± 7.3	± 13.0	± 11.0	+19.0 -18.0	
-0.40, +0.40	± 3.1	+5.8 -5.7	± 4.4	+8.2 -8.4	± 3.3	+6.3 -6.2	+4.5 -5.2	+9.3 -8.5	
0.00, 0.00	± 1.7	± 3.3	± 2.5	± 4.8	± 1.9	+3.7 -3.6	+2.3 -2.7	+5.1 -4.6	Unpolarized point
+0.09, -0.10	± 1.7	± 3.2	± 2.4	+4.7 -4.6	± 1.8	+3.5 -3.4	+2.2 -2.6	+4.9 -4.5	$P_{Z\gamma}$, best-choice for $Z\gamma$
+0.12, -0.12	± 1.6	± 3.1	± 2.4	± 4.7	± 1.8	+3.5 -3.4	+2.2 -2.6	+5.0 -4.5	P_{best} , combined best-choice
+0.16, -0.16	± 1.6	± 3.1	± 2.4	± 4.7	± 1.8	+3.5 -3.4	+2.3 -2.7	+5.1 -4.5	P_{ZZ} , best-choice for ZZ
+0.40, -0.40	± 1.9	± 3.7	± 3.2	+6.1 -6.2	± 2.1	+4.0 -4.1	+3.1 -3.7	+6.7 -6.0	
+0.80, -0.80	+5.3 -6.2	+9.8 -9.3	+9.7 -12.0	+18.0 -17.0	± 5.4	+9.5 -9.9	± 9.9	+17.0 -18.0	

Table 2 List of simultaneous limits on anomalous couplings obtained for $\sqrt{s} = 500$ GeV and $L = 100$ fb $^{-1}$ for different η_3 and ξ_3 from MCMC in Z γ process

Beam polarizations	Limits on couplings (10^{-3})								Comments
	h_1^γ		h_1^Z		h_3^γ		h_3^Z		
(η_3, ξ_3)	68 %	95 %	68 %	95 %	68 %	95 %	68 %	95 %	
-0.80, +0.80	+7.7 -9.3	± 13.0	± 11.0	+18.0 -19.0	± 7.5	± 13.0	± 11.0	± 19.0	
-0.40, +0.40	± 3.9	+7.4 -7.5	± 6.5	± 12.0	+4.4 -3.7	+7.1 -8.0	± 6.6	+13.0 -12.0	
0.00, 0.00	± 1.6	± 3.1	± 3.7	+7.1 -7.0	+1.6 -1.4	+2.8 -3.0	± 3.6	± 7.1	Unpolarized point
+0.09, -0.10	± 1.5	± 2.9	± 3.6	± 7.0	+1.4 -1.3	+2.6 -2.8	± 3.6	+7.0 -7.1	$P_{Z\gamma}$, best-choice for $Z\gamma$
+0.12, -0.12	± 1.5	± 2.9	± 3.7	± 7.1	± 1.4	+2.6 -2.8	± 3.6	± 7.1	P_{best} , combined best-choice
+0.16, -0.16	± 1.5	± 3.0	± 3.7	+7.2 -7.3	+1.5 -1.3	+2.6 -2.8	± 3.7	+7.1 -7.3	P_{ZZ} , best-choice for ZZ
+0.40, -0.40	± 2.4	± 4.6	± 5.2	± 10.0	+2.5 -2.2	+4.3 -4.7	± 5.2	± 10.0	
+0.80, -0.80	± 5.8	+10.0 -9.9	+11.0 -13.0	+19.0 -18.0	+5.8 -7.2	+10.0 -9.7	+13.0 -15.0	+19.0 -18.0	

in Eq. 13. The combined averaged likelihood showing dependence on the beam polarizations for the two processes considered here is shown in Fig. 7. The dot on the middle of the plot is for the unpolarized case and asterisk mark at $P_{best} = (+0.12, -0.12)$ is the combined best-choice of beam polarizations. Other points are due to P_{ZZ} and $P_{Z\gamma}$. The combined best-choice point sits in between P_{ZZ} and $P_{Z\gamma}$. The limits, presented in Table 1 and 2, at the combined best-choice of the beam polarizations are slightly weaker than the limit at the best-choice points but comparable in both processes as expected. Thus the combined best-choice can be a good benchmark beam polarizations for the process ZZ and $Z\gamma$ to study at ILC.

The best-choice of beam polarizations, obtained here, depends on the size of the estimated error of the observables and hence on the systematics ϵ_σ and ϵ_A . Numerical analysis shows that the best-choice points, for both processes separately and combined, move away from the unpolarized point along the cross diagonal axis towards the right-bottom corner on the $\eta_3 - \xi_3$ plane when ϵ_σ or ϵ_A or both are increased. For example, if we double ϵ_σ and ϵ_A both, i.e. we take $\epsilon_\sigma = 0.04$ and $\epsilon_A = 0.02$, the best-choice points P_{ZZ} , $P_{Z\gamma}$ and P_{best} become $(+0.20, -0.20)$, $(+0.13, -0.12)$ and $(+0.17, -0.16)$, respectively. On the other hand the best-choice points move towards the unpolarized point as the systematics are decreased. For example, when the

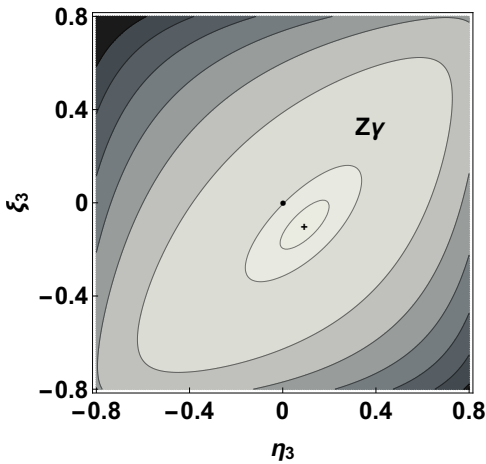


Fig. 6 Same as Fig. 5 but for the $Z\gamma$ process. The plus mark at $P_{Z\gamma} = (+0.09, -0.10)$ is the lowest likelihood point and hence the best-choice of beam polarizations for $Z\gamma$ process

systematics are reduced by 1/2, i.e. for $\varepsilon_\sigma = 0.01$ and $\varepsilon_A = 0.005$, the best-choice points for ZZ , $Z\gamma$ and for combined process move to $(+0.15, -0.15)$, $(+0.08, -0.08)$ and $(+0.11, -0.11)$, respectively. However, the best-choice points do not move further closer to the unpolarized point when the size of systematics becomes smaller than the statistical one.

Similar analysis as presented in Fig. 7 can be done by combining many processes, as one should do, to choose a suitable beam polarizations at ILC. For many processes (e.g., we can include WW production with anomalous couplings among charged gauge boson) with different couplings, the volume in which one should do the average will change to $V_{\mathbf{f}/\mathbf{h}} = V_{\mathbf{F}}$, where \mathbf{F} would be the set of all couplings for all the processes considered. The set of observables $\{\mathcal{O}\}$ would include all the relevant observables from all the processes combined in the expression for the likelihood.

4 Conclusion

To summarize, we aim to find the best-choice of beam polarization for an e^+e^- collider to probe the anomalous couplings in the neutral gauge-boson sector in the ZZ and $Z\gamma$ processes. We study the effects of beam polarization on polarization asymmetries and corresponding sensitivities towards anomalous couplings. Using the *minimum averaged* likelihood, we find the best-choice of the beam polarization for the two processes and also the combined best-choice. Here the list of observables includes the cross section along with eight polarization asymmetries for the Z boson. Simultaneous limits on anomalous couplings were obtained using the MCMC method for a set of benchmark beam polarization including the best-choices and they are listed in

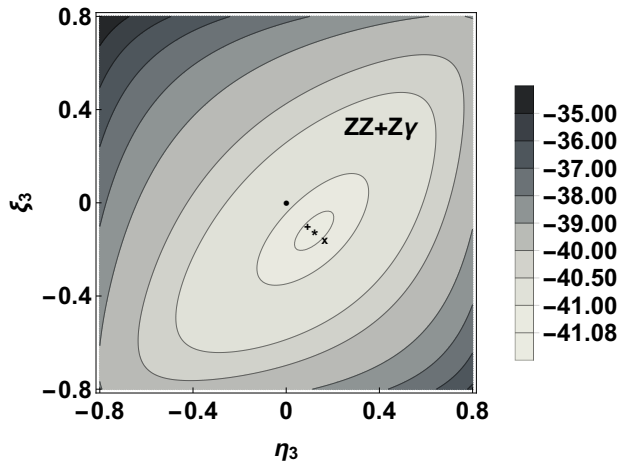


Fig. 7 The log of average likelihood, $\log[L(V_{\mathbf{f}/\mathbf{h}}, \{\mathcal{O}\}; \eta_3, \xi_3)]$, is shown considering both the processes ZZ and $Z\gamma$ at $\sqrt{s} = 500$ GeV, $\mathcal{L} = 100$ fb $^{-1}$. The asterisk mark at $P_{best} = (+0.12, -0.12)$ is the combined best-choice for beam polarizations while the other points are for ZZ (cross mark) and $Z\gamma$ (plus mark)

Tables 1 and 2. The limits obtained for the unpolarized case are better than the ones reported in Ref. [28]. This is because the present analysis includes three new observables \tilde{A}_z , \tilde{A}_{xz} and \tilde{A}_{yz} . These new asymmetries yield better limits on $f_{4,5}^Z$ and $h_{1,3}^Z$, while we have comparable (yet better) limits on $f_{4,5}^\gamma$ and $h_{1,3}^\gamma$. Comparing the limits for various benchmark beam polarizations from Tables 1 and 2, we find that all three *best* beam polarization choices yield comparable limits and they are comparable to the unpolarized case as well. Thus, as far as anomalous couplings in the neutral gauge-boson sector are concerned, unpolarized beams perform as good as the *best* choices. This conclusion, however, can change if one includes more or a different set of observables in the analysis or add more processes to the analysis. For example, processes involving W^\pm or a Higgs boson may have a different preference for the beam polarization.

Considering the physics impact and the cost of beam polarizations at ILC one may chose the unpolarized beams for the first run, at least for the two processes studied here. But as we infer, a detailed global analysis is required involving other processes as well to conclude this. We further note that the case of transverse beam polarization is not addressed here and conclusions may differ in that case.

Acknowledgements: R. R. thanks Department of Science and Technology, Government of India for support through DST-INSPIRE Fellowship for doctoral program, INSPIRE CODE IF140075, 2014.

References

1. **CMS** Collaboration, S. Chatrchyan *et al.*, Observation of a new boson at a mass of 125 GeV with the CMS experiment at

- the LHC, *Phys. Lett.* **B716** (2012) 30–61, [arXiv:1207.7235 \[hep-ex\]](#).
2. ILC Collaboration, G. Aarons *et al.*, International Linear Collider Reference Design Report Volume 2: Physics at the ILC, [arXiv:0709.1893 \[hep-ph\]](#).
 3. H. Baer, T. Barklow, K. Fujii, Y. Gao, A. Hoang, S. Kanemura, J. List, H. E. Logan, A. Nomerotski, M. Perelstein, *et al.*, The International Linear Collider Technical Design Report - Volume 2: Physics, [arXiv:1306.6352 \[hep-ph\]](#).
 4. T. Behnke, J. E. Brau, B. Foster, J. Fuster, M. Harrison, J. M. Paterson, M. Peskin, M. Stanitzki, N. Walker, and H. Yamamoto, The International Linear Collider Technical Design Report - Volume 1: Executive Summary, [arXiv:1306.6327 \[physics.acc-ph\]](#).
 5. G. Moortgat-Pick *et al.*, The Role of polarized positrons and electrons in revealing fundamental interactions at the linear collider, *Phys. Rept.* **460** (2008) 131–243, [arXiv:hep-ph/0507011 \[hep-ph\]](#).
 6. V. V. Andreev, G. Moortgat-Pick, P. Osland, A. A. Pankov, and N. Paver, Discriminating Z' from Anomalous Trilinear Gauge Coupling Signatures in $e^+e^- \rightarrow W^+W^-$ at ILC with Polarized Beams, *Eur. Phys. J.* **C72** (2012) 2147, [arXiv:1205.0866 \[hep-ph\]](#).
 7. B. Ananthanarayan, M. Patra, and P. Poullose, Signals of additional Z boson in $e^+e^- \rightarrow W^+W^-$ at the ILC with polarized beams, *JHEP* **02** (2011) 043, [arXiv:1012.3566 \[hep-ph\]](#).
 8. P. Osland, A. A. Pankov, and A. V. Tsytinov, Identification of extra neutral gauge bosons at the International Linear Collider, *Eur. Phys. J.* **C67** (2010) 191–204, [arXiv:0912.2806 \[hep-ph\]](#).
 9. A. A. Pankov, N. Paver, and A. V. Tsytinov, Distinguishing new physics scenarios at a linear collider with polarized beams, *Phys. Rev.* **D73** (2006) 115005, [arXiv:hep-ph/0512131 \[hep-ph\]](#).
 10. O. Kittel, G. Moortgat-Pick, K. Rolbieceki, P. Schade, and M. Terwort, Measurement of CP asymmetries in neutralino production at the ILC, *Eur. Phys. J.* **C72** (2012) 1854, [arXiv:1108.3220 \[hep-ph\]](#).
 11. H. K. Dreiner, O. Kittel, and A. Marold, Normal tau polarisation as a sensitive probe of CP violation in chargino decay, *Phys. Rev.* **D82** (2010) 116005, [arXiv:1001.4714 \[hep-ph\]](#).
 12. A. Bartl, K. Hohenwarter-Sodek, T. Kernreiter, and O. Kittel, CP asymmetries with longitudinal and transverse beam polarizations in neutralino production and decay into the Z0 boson at the ILC, *JHEP* **09** (2007) 079, [arXiv:0706.3822 \[hep-ph\]](#).
 13. K. Rao and S. D. Rindani, Probing CP-violating contact interactions in $e^+e^- \rightarrow \gamma Z$ with polarized beams, *Phys. Lett.* **B642** (2006) 85–92, [arXiv:hep-ph/0605298 \[hep-ph\]](#).
 14. A. Bartl, H. Fraas, S. Hesselbach, K. Hohenwarter-Sodek, T. Kernreiter, and G. A. Moortgat-Pick, CP-odd observables in neutralino production with transverse e^+ and e^- beam polarization, *JHEP* **01** (2006) 170, [arXiv:hep-ph/0510029 \[hep-ph\]](#).
 15. H. Czyz, K. Kolodziej, and M. Zralek, Composite Z Boson and CP Violation in the Process $e^+e^- \rightarrow Z\gamma$, *Z. Phys.* **C43** (1989) 97.
 16. D. Choudhury and S. D. Rindani, Test of CP violating neutral gauge boson vertices in $e^+e^- \rightarrow \gamma Z$, *Phys. Lett.* **B335** (1994) 198–204, [arXiv:hep-ph/9405242 \[hep-ph\]](#).
 17. B. Ananthanarayan, S. D. Rindani, R. K. Singh, and A. Bartl, Transverse beam polarization and CP-violating triple-gauge-boson couplings in $e^+e^- \rightarrow \gamma Z$, *Phys. Lett.* **B593** (2004) 95–104, [arXiv:hep-ph/0404106 \[hep-ph\]](#). [Erratum: *Phys. Lett.* **B608**,274(2005)].
 18. B. Ananthanarayan, S. K. Garg, M. Patra, and S. D. Rindani, Isolating CP-violating γZZ coupling in $e^+e^- \rightarrow \gamma Z$ with transverse beam polarizations, *Phys. Rev.* **D85** (2012) 034006, [arXiv:1104.3645 \[hep-ph\]](#).
 19. B. Ananthanarayan and S. D. Rindani, CP violation at a linear collider with transverse polarization, *Phys. Rev.* **D70** (2004) 036005, [arXiv:hep-ph/0309260 \[hep-ph\]](#).
 20. S. Groote, J. G. Korner, B. Melic, and S. Prelovsek, A survey of top quark polarization at a polarized linear e^+e^- collider, *Phys. Rev.* **D83** (2011) 054018, [arXiv:1012.4600 \[hep-ph\]](#).
 21. M. S. Amjad *et al.*, A precise characterisation of the top quark electro-weak vertices at the ILC, *Eur. Phys. J.* **C75** no. 10, (2015) 512, [arXiv:1505.06020 \[hep-ex\]](#).
 22. B. Ananthanarayan, M. Patra, and P. Poullose, W physics at the ILC with polarized beams as a probe of the Littlest Higgs Model, *JHEP* **11** (2009) 058, [arXiv:0909.5323 \[hep-ph\]](#).
 23. B. Ananthanarayan, M. Patra, and P. Poullose, Probing strongly interacting W's at the ILC with polarized beams, *JHEP* **03** (2012) 060, [arXiv:1112.5020 \[hep-ph\]](#).
 24. S. Kumar, P. Poullose, and S. Sahoo, Study of Higgs-gauge boson anomalous couplings through $e^-e^+ \rightarrow W^-W^+H$ at ILC, *Phys. Rev.* **D91** no. 7, (2015) 073016, [arXiv:1501.03283 \[hep-ph\]](#).
 25. S. D. Rindani and P. Sharma, Decay-lepton correlations as probes of anomalous ZZH and gammaZH interactions in $e^+e^- \rightarrow \gamma Z$ with polarized beams, *Phys. Lett.* **B693** (2010) 134–139, [arXiv:1001.4931 \[hep-ph\]](#).
 26. S. S. Biswal and R. M. Godbole, Use of transverse beam polarization to probe anomalous VVH interactions at a Linear Collider, *Phys. Lett.* **B680** (2009) 81–87, [arXiv:0906.5471 \[hep-ph\]](#).
 27. S. D. Rindani and P. Sharma, Angular distributions as a probe of anomalous ZZH and gammaZH interactions at a linear collider with polarized beams, *Phys. Rev.* **D79** (2009) 075007, [arXiv:0901.2821 \[hep-ph\]](#).
 28. R. Rahaman and R. K. Singh, On polarization parameters of spin-1 particles and anomalous couplings in $e^+e^- \rightarrow ZZ/Z\gamma$, *Eur. Phys. J.* **C76** no. 10, (2016) 539, [arXiv:1604.06677 \[hep-ph\]](#).
 29. F. Boudjema and R. K. Singh, A Model independent spin analysis of fundamental particles using azimuthal asymmetries, *JHEP* **07** (2009) 028, [arXiv:0903.4705 \[hep-ph\]](#).
 30. J. A. Aguilar-Saavedra and J. Bernabeu, Breaking down the entire W boson spin observables from its decay, *Phys. Rev.* **D93** no. 1, (2016) 011301, [arXiv:1508.04592 \[hep-ph\]](#).
 31. F. Boudjema, Proc. of the Workshop on e^-e^+ Collisions at 500GeV: The Physics Potential, edited by P.M. Zerwas, *DESY* (1992) 757.
 32. U. Baur and E. L. Berger, Probing the weak boson sector in $Z\gamma$ production at hadron colliders, *Phys. Rev.* **D47** (1993) 4889–4904.
 33. J. Ellison and J. Wudka, Study of trilinear gauge boson couplings at the Tevatron collider, *Ann. Rev. Nucl. Part. Sci.* **48** (1998) 33–80, [arXiv:hep-ph/9804322 \[hep-ph\]](#).
 34. U. Baur and D. L. Rainwater, Probing neutral gauge boson selfinteractions in ZZ production at hadron colliders, *Phys. Rev.* **D62** (2000) 113011, [arXiv:hep-ph/0008063 \[hep-ph\]](#).
 35. B. Ananthanarayan and S. D. Rindani, New physics in $e^+e^- \rightarrow Z\gamma$ with polarized beams, *JHEP* **10** (2005) 077, [arXiv:hep-ph/0507037 \[hep-ph\]](#).

-
36. H. Aihara *et al.*, Anomalous gauge boson interactions, [arXiv:hep-ph/9503425](#) [hep-ph].
 37. G. J. Gounaris, J. Layssac, and F. M. Renard, Off-shell structure of the anomalous Z and γ selfcouplings, *Phys. Rev.* **D65** (2002) 017302, [arXiv:hep-ph/0005269](#) [hep-ph]. [*Phys. Rev.*D62,073012(2000)].
 38. P. Poulose and S. D. Rindani, CP violating $Z\gamma\gamma$ and top quark electric dipole couplings in $\gamma\gamma \rightarrow t\bar{t}$, *Phys. Lett.* **B452** (1999) 347–354, [arXiv:hep-ph/9809203](#) [hep-ph].
 39. A. Senol, $ZZ\gamma$ and $Z\gamma\gamma$ anomalous couplings in γp collision at the LHC, *Phys. Rev.* **D87** (2013) 073003, [arXiv:1301.6914](#) [hep-ph].
 40. I. Ots, H. Uibo, H. Liivat, R. Saar, and R. K. Loide, Possible anomalous $Z Z$ gamma and Z gamma gamma couplings and Z boson spin orientation in $e^+e^- \rightarrow Z\gamma$: The role of transverse polarization, *Nucl. Phys.* **B740** (2006) 212–221.
 41. B. Ananthanarayan, J. Lahiri, M. Patra, and S. D. Rindani, New physics in $e^+e^- \rightarrow Z\gamma$ at the ILC with polarized beams: explorations beyond conventional anomalous triple gauge boson couplings, *JHEP* **08** (2014) 124, [arXiv:1404.4845](#) [hep-ph].
 42. G. J. Gounaris, J. Layssac, and F. M. Renard, Signatures of the anomalous Z_γ and ZZ production at the lepton and hadron colliders, *Phys. Rev.* **D61** (2000) 073013, [arXiv:hep-ph/9910395](#) [hep-ph].
 43. S. Y. Choi, Probing the weak boson sector in $\gamma e \rightarrow Ze$, *Z. Phys.* **C68** (1995) 163–172, [arXiv:hep-ph/9412300](#) [hep-ph].
 44. T. G. Rizzo, Polarization asymmetries in gamma e collisions and triple gauge boson couplings revisited, in *Physics and experiments with future linear e^+e^- colliders. Proceedings, 4th Workshop, LCWS'99, Sitges, Spain, April 28-May 5, 1999. Vol. 1: Physics at linear colliders*, pp. 529–533. 1999. [arXiv:hep-ph/9907395](#) [hep-ph]. <http://www-public.slac.stanford.edu/sciDoc/docMeta.aspx?slacPubNumber=SLAC-PUB-8192>.
 45. S. Atag and I. Sahin, ZZ gamma and Z gamma gamma couplings in gamma e collision with polarized beams, *Phys. Rev.* **D68** (2003) 093014, [arXiv:hep-ph/0310047](#) [hep-ph].
 46. CMS Collaboration, V. Khachatryan *et al.*, Measurements of the $Z Z$ production cross sections in the $2l2\nu$ channel in protonproton collisions at $\sqrt{s} = 7$ and 8 TeV and combined constraints on triple gauge couplings, *Eur. Phys. J.* **C75** no. 10, (2015) 511, [arXiv:1503.05467](#) [hep-ex].
 47. ATLAS Collaboration, G. Aad *et al.*, Measurements of $Z\gamma$ and $Z\gamma\gamma$ production in pp collisions at $\sqrt{s} = 8$ TeV with the ATLAS detector, *Phys. Rev.* **D93** no. 11, (2016) 112002, [arXiv:1604.05232](#) [hep-ex].